RSC Advances

ROYAL SOCIETY OF CHEMISTRY

www.rsc.org/advances

The activation of N-glycosidic bond cleavage operated by base-excision repair enzyme hOGG1; theoretical study of the role of Lys 249 residue in activation of G, OxoG and FapyG

Jakub Šebera[1], Lukáš Trantírek[2], Yoshiyuki Tanaka[3], Radim Nencka[1], Jiří Fukal[1], and Vladimír Sychrovský[1]*

[1] Institute of Organic Chemistry and Biochemistry AS CR, v.v.i., Flemingovo náměstí 2, 16610 Praha, Czech Republic

[2] Central European Institute of Technology – Masaryk University, Kamenice 753/5, 625 00 Brno, Czech Republic

[3] Division of Pharmaceutical Chemistry, Tohoku University, Aobayama, Aoba-ku, Sendai, Miyagi 980-8578 Japan

*To whom correspondence should be addressed:
Dr. Vladimír Sychrovský
Institute of Organic Chemistry and Biochemistry AS CR, v.v.i.
Flemingovo náměstí 2, 16610 Praha, Czech Republic
Phone: 00420 220183234
Email: vladimir.sychrovsky@uochb.cas.cz

Keywords: 8-oxo-2'-deoxyguanosine, hOGG1, N-glycosidic Bond, DNA Glycosylase, Base Excision Repair, Enzyme Catalysis

† Electronic supplementary information (ESI) available: Calculated molecular properties and geometric parameters in Tables S1-S15 and Figure S1-S8.

Abstract

The activation of N-glycosidic bond cleavage operated by lysine 249 (Lys 249) residue of base-excision repair enzyme hOGG1 was calculated for 2′-deoxyguanosine (G), 8-oxo-2'-deoxyguanosine (OxoG) and N6-(2'-β-D-deoxyribofuranosyl)-2,6-diamino-4-hydroxy-5-formamidopyrimidine (FapyG). The interaction sites of Lys 249 included C1', N3, and N9 atoms of the nucleosides. The N9-pathway, specifically the attack of lone-pair electrons at glycosidic nitrogen N9 of a nucleoside to proton of Nε-ammonium of Lys 249, resulted in effective activation of C1'-N9 bond that was highly specific with respect to normal (G) and damaged (OxoG, FapyG) nucleosides. The specificity of N9-pathway was owing to electrophilic (G) or nucleophilic (OxoG, FapyG) character of the glycosidic nitrogen and owing to specific interactions of the residues within catalytic pocket with substrate (particularly the Gly 42 hOGG1 residue) that enforced displacement of G out of interaction range of Lys 249. The chemical modifications of G owing to damage affected specifically number of molecular properties including particularly electrophilicity/nucleophilicity of N9, C1'-N9 bond order and aromatic character of nucleobase. The N9-pathway could be involved as a check-point mechanism during base-excision operated by hOGG1.

Introduction

The repair of DNA is necessary because genetic material may be altered owing to pollutants and some chemical compounds that occur normally in the cell. The damaged DNA must be repaired otherwise it may cause serious damage of organism. Extreme efficiency and specificity of the DNA repair with respect to particular kind of damage is ensured by base-excision repair enzymes (BER enzymes).[1,2]

The BER enzyme targeting specifically 8-oxo-2'-deoxyguanosine (OxoG) that is produced owing to oxidation of normal 2′-deoxyguanosine (G), is called human 8-oxoguanine glycosylase 1 (hOGG1).[3,4,5,6,7,8,9,10,11,12] The repair mechanism operated by hOGG1 was described generally.[13,14] The excision of OxoG base is initiated by formation of DNA-hOGG1 conjugate involving interaction of lysine 249 residue (Lys 249) with OxoG that is extruded out of double helix and dipped into the hOGG1 catalytic pocket.[1,3,15] After OxoG elimination, the pathway continues by formation of a Schiff base and the repair process terminates by cleavage of a defective DNA strand. The mechanism of excision of OxoG is currently unclear despite that the structure of catalytic pocket including substrate nucleoside is known. The role of residues within hOGG1 catalytic pocket including Lys 249 remained unknown.[16,17,18,19] The original base-excision S_N1 or S_N2-type mechanisms were proposed based on crystallographic and biochemical data.[3,13,14,18,17] The theoretical modeling of excision pathways was aimed particularly at role of hOGG1 residues during OxoG excision.[20,21,22,23,24,25,26]

The recognition of OxoG lesions by hOGG1 is extremely specific.[1] Consecutive check of the individual nucleobases within hOGG1 catalytic pocket is not assumed, however, the DNA-hOGG1 complex containing flipped out normal G can be formed transiently.[27] Moreover, the existence of unknown check-point mechanism responsible for distinguishing OxoG from G was reported.[28] Although normal G was enforcedly inserted into hOGG1 catalytic pocket the base excision was not observed.[28] The peculiar check-point mechanism might therefore recognize case-selectively some local property of a substrate nucleoside. With that goal in mind, the interactions of Lys 249 with three model nucleosides were studied in this work.

The specific stabilization and activation of a substrate within catalytic site is typical strategy common to all enzymes, not excluding the BER enzymes.[1,29] In this respect, the pre-protonation of a nucleobase activates N-glycosidic bond cleavage because negative charge of nucleobase during excision is compensated. The proton addition to O8 oxygen[20], N3 nitrogen[30], and N9 glycosidic nitrogen[31] of OxoG were modeled theoretically previously.

The interaction of protonated Lys 249 with glycosidic nitrogen of OxoG enforced distinct pyramidal geometry of N9 (N9-pyramidalization) and shifted its electronic state from sp^2-like more toward sp^3-like, which allowed substitution of N-glycosidic bond with N9-H bond.[31] The pyramidal geometry of glycosidic nitrogen was observed in crystal structures of normal DNA and RNA molecules previously.[32] The N9-pyramidalization of G residues within DNA G-quadruplex was enforced by surrounding molecules.[33] The N9-pyramidalization of model nucleosides was studied in this work as a key structural descriptor of one of the base-excision pathways.

The previous calculations of N-glycosidic bond cleavage unveiled that Lys 249 may interact with OxoG and normal G differently.[31] In particular, the electronic state of glycosidic nitrogen might allow or block

its interaction with Lys 249. To analyze such check-point mechanism in detail we focused on properties of the G, OxoG and N6-(2'-β-D-deoxyribofuranosyl)-2,6-diamino-4-hydroxy-5-formamidopyrimidine (FapyG) nucleosides (Figure 1). Out of the three nucleosides only OxoG and FapyG are cleavable with hOGG1 and better cleavability was observed for FapyG.[18,17,34] The theoretical study on activation of N-gycosidic bond is therefore well-founded by experimental observations.

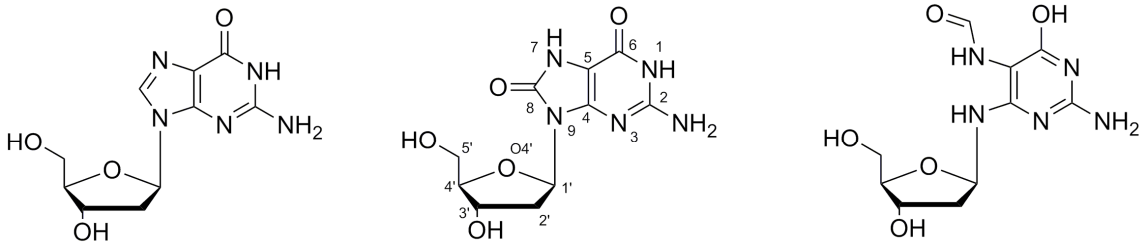

Figure 1. The chemical structure of 2′-deoxyguanosine (G), 8-oxo-2'-deoxyguanosine (OxoG) and N6-(2'-β-D-deoxyribofuranosyl)-2,6-diamino-4-hydroxy-5-formamidopyrimidine (FapyG) nucleoside. The atom numbering used in text was depicted only for OxoG. The sugar-to-base orientation was measured with the glycosidic torsion angle χ = C4-N9-C1'-O4 and the extent of N9-pyramidalization was measured employing torsion angle κ' = C4-N9-C1'-C8 - 180° (G, OxoG) or κ' = C4-N9-C1´-H9 - 180° (FapyG).

Results and discussion

The Lys 249 is key hOGG1 residue, however, its exact role during base excision is currently unknown. The two basic-excision pathways employing Lys 249 were proposed based on pioneering x-ray structural data.[17] The classical scheme assumed for BER enzymes is in the case of hOGG1 initiated by neutral Lys 249, specifically owing to interaction of Nε-amino group of Lys 249 with C1' anomeric carbon of OxoG.[13,14,3,5,18] The reaction of Lys 249 with nucleoside that initiates S_N2 reaction will be called C1'-pathway (Figure 2). The protonated Lys 249 was suggested to stabilize leaving nucleobase after its excision owing to interaction of cationic Nε-ammonium of Lys 249 with anionic OxoG base.[1,17] The actual state of Lys 249 during excision is currently unknown, however, the occurrence of protonated form was assumed previously based on experimental NMR data.[20]

The pre-protonation of nucleobase enhances its excision. Several reactions employing this strategy were proposed and calculated previously. The stabilization of cleaved OxoG base with Nε-ammonium of Lys 249 was calculated by Schyman and coworkers.[21] The proton addition to O8 oxygen of OxoG was calculated by Osakabe and coworkers.[20] This scheme was not included in this work because: a) the activation energy of OxoG excision (42 kcal mol^{-1})[20] was significantly higher than values expected for BER enzymes (≈19 kcal mol^{-1})[1] and b) the direct contact of O8 oxygen with Nε-ammonium of Lys 249 would be hardly possible owing to O8 - Nε distance (4.74 Å and 4.34 Å, the x-ray structure 1N3C and 2NOZ). The proton addition to N3 nitrogen as a mode of N-glycosidic bond activation was proposed by Jang and coworkers.[35] The

protonation of N3 nitrogen of OxoG by deprotonation of Nε-ammonium of Lys 249 was calculated by Calvaresi and coworkers.[30] This initial reaction of Lys 249 resulting again in S_N2 reaction pathway (after N3 protonation the reaction continues via C1'-pathway) will be called N3-pathway (Figure 2). The effect of protonated glycosidic nitrogen on hydrolytic cleavage of N-glycosidic bond was calculated by Cysewski and coworkers.[36] The strong activation of hydrolytic cleavage was concluded but protonation of N9 was considered practically impossible owing to its very low basicity.[36] The attack of lone-pair electrons at glycosidic nitrogen to proton of Nε-ammonium of Lys 249 that allowed proton addition to N9 during cleavage of N-glycosidic bond of OxoG was calculated by Šebera and coworkers.[31] The interaction of Lys 249 with N9 nitrogen (N9-pathway, Figure 2) is equally possible as the interactions with C1' and N3 atoms of OxoG. The distances between Nε nitrogen of Lys 249 and N9, N3, and C1' atoms of OxoG ranged 3.0 ÷ 3.5 Å in the x-ray structures 1N3C and 2NOZ. The cleavage of N-glycosdic bond of OxoG employing C1'-pathway, N3-pathway, and N9-pathway were calculated previously and the lowest activation energy was obtained for N9-pathway.[31]

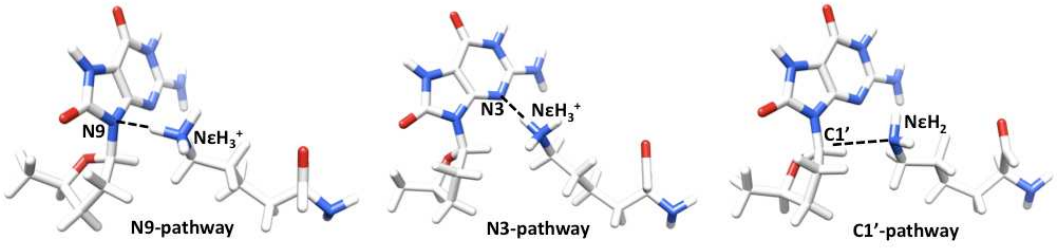

Figure 2. The initiation of reaction pathways operated by Lys 249 hOGG1 residue as described employing small model (see Computational details): the N9-pathway assumes interaction of Nε-ammonium (Lys 249) with glycosidic nitrogen N9, the N3-pathway assumes interaction of Nε-ammonium with N3 nitrogen, and the C1'-pathway assumes interaction of Nε-amino group of Lys 249 with C1' anomeric carbon.

The optimized geometries of G, OxoG, and FapyG nucleosides calculated employing small model were different. The length of N-glycosidic bond ($r_{C1'-N9}$) of G, OxoG, and FapyG was 1.468 Å, 1.456 Å, and 1.446 Å and the κ' torsion angle was -3.1°, 10.5°, and 30.3°, respectively. The C1'-N9 bond of damaged nucleosides shrank as compared to normal G and N9-pyramidalization increased. The $r_{C1'-N9}$ shrank upmost by 0.008 Å and the N9-pyramidalization changed only a little owing to C1'-pathway (Table 1). The $r_{C1'-N9}$ of FapyG lengthened by 0.018 Å and N9-pyramidalization of OxoG and FapyG increased owing to N3-pathway (Table 1). The initiation of N3-pathway may continue with proton transfer from Nε-ammonium to N3 nitrogen that was calculated for all three nucleosides. The $r_{C1'-N9}$ and N9-pyramidalization were practically not affected by the proton transfer (Table 1).

The N9-pathway reaction was calculated only for OxoG and FapyG. The stationary point describing respective interaction of G with Lys 249 was not calculated and all the attempts of geometry optimizations resulted in N3-pathway reaction (data not shown). The N9-pathway with proton transferred to N9 nitrogen was calculated only for FapyG. The $r_{C1'-N9}$ of OxoG and FapyG lengthened owing to N9-pathway by 0.023 Å and by 0.034 Å, respectively, and by 0.068 Å owing to proton transfer to N9 of FapyG. The κ' torsion of OxoG and FapyG increased owing to N9-pathway by 27.3° and 19.6°, respectively, and by 27.7° owing to proton transfer to N9 of FapyG (Table 1). The N9-pathway affected key geometric parameters of OxoG and FapyG more than other two pathways. The lengthening of N-glycosidic bond and the increase of N9-pyramidalization were marked changes indicative of activation of N-glycosidic bond.

Table 1. The calculated geometric parameters and bond orders of free nucleosides and nucleosides interacting with Lys 249.[a)]

Parameter[b)]	Free nucleoside	C1'-pathway	N3-pathway		N9-pathway	
	G	G (C1')	G (N3)	G (N3H)	G (N9)	G (N9H)
$r_{C1'-N9}$	1.468	1.460	1.461	1.471	-	-
C1´-N9	0.898	0.908	0.913	0.897	-	-
κ'	-3.1	-3.8	1.5	2.3	-	-
	OxoG	OxoG (C1')	OxoG (N3)	OxoG (N3H)	OxoG (N9)	OxoG (N9H)
$r_{C1'-N9}$	1.456	1.454	1.458	1.464	1.479	-
C1´-N9	0.924	0.922	0.923	0.912	0.905	-
κ'	10.5	2.6	17.1	18.4	37.8	-
	FapyG	FapyG (C1')	FapyG (N3)	FapyG (N3H)	FapyG (N9)	FapyG (N9H)
$r_{C1'-N9}$	1.446	1.446	1.463	1.464	1.480	1.514
C1´-N9	0.971	0.969	0.957	0.947	0.929	0.867
κ'	30.3	31.6	41.9	38.3	49.6	58.0

[a)] The interaction of Lys 249 with nucleoside is indicated in parenthesis as follows: C1'-pathway (C1'), N3-pathway (N3), N3-pathway with proton transferred from Nε-ammonium to N3 nitrogen (N3H), N9-pathway (N9), N9-pathway with proton transferred from Nε-ammonium to N9 nitrogen (N9H). [b)] The $r_{C1'-N9}$ bond length in Å, the C1´-N9 bond order, and the κ' torsion angle in degrees (the definition of κ' can be found in Figure 1). The calculations were done employing small model depicted in Figure 2 and described in Computational details. -: not calculated (see the text).

The calculations employing medium and large models unveiled effect of hOGG1 residues within catalytic pocket on activation of N-glycosidic bond (Figure 3). The calculated glycosidic torsion angles χ of nucleosides ranged 248.7°÷290.5°, which was in agreement with the *anti* orientation of OxoG and G in x-ray structures (Table S4). The $r_{C1'-N9}$ of nucleosides within catalytic pocket (medium model) and $r_{C1'-N9}$ of free nucleosides (small model) decreased in the same order that was coherent with x-ray structural data (Table 1,

Table S4). The damage of G affected intrinsic properties of N-glycosidic bond. The length of glycosidic bond of damaged nucleosides is shorter.

The QM/MM calculations employing large model indicated relatively ordered catalytic core and Nε-ammonium of Lys 249 closer to N9 atom of OxoG than to N3 or C1' atoms of OxoG (Tables S4). The CAM-B3LYP calculations employing medium model unveiled distinct initiation of N9-pathway in the case of OxoG and FapyG while in the case of G was initiated rather N3-pathway. The Nε-N9 distance calculated for G, OxoG, and FapyG was 3.629 Å, 3.021 Å, 2.777 Å and the Nε-N3 distance was 2.704 Å, 3.425 Å, and 3.260 Å. The x-ray structures unveiled catalytic pocket containing G more opened as compared to pocket containing OxoG (Table S4). The calculations and x-ray geometries indicated consistently initiation of N9-pathway in the case of OxoG and N3-pathway in the case of G.

The catalytic pocket containing G was corrupted and G nucleoside was displaced from Lys 249. The activation of N-glycosidic bond of G employing Lys 249 was therefore less possible. The adjustment of catalytic core in response to inserted nucleobase was substrate-specific. Among hOGG1 residues within catalytic site the Gly 42 interacted specifically with normal and damaged nucleosides. The H-bond between oxygen of Gly 42 and H7 hydrogen stabilized positioning of OxoG and FapyG (Figure 3) while in the case of G repulsion between oxygen of Gly 42 and N7 nitrogen occurred. The calculations and x-ray structures indicated coherently key role of Gly 42 in freezing well-defined position of damaged nucleoside within catalytic pocket.

The N9-pyramidalizations of OxoG and FapyG calculated employing medium and small models were similar since the κ' torsions differed less than 1.4° (Table 1 and Table S4). On the contrary, the N9-pyramidalization of G within catalytic pocket (medium model, κ' = 29.9°) was notably larger than N9-pyramidalizations of G calculated employing small model (κ' = -3.1° ÷ 2.3°, Table 1). The peculiar N9-pyramidalization of G within catalytic pocket was rationalized. First, the deformation energy needed for enforcement of the N9-pyramidalization (κ' ≈ 30°) should be only ca 1.5 kcal·mol^{-1}.[33] Second, the starting geometry of G employed in geometry optimization was derived from the x-ray structure 2NOZ that showed close proximity of OxoG to Lys 249 and particularly effective H-bond of OxoG with Gly 42. The N9-pyramidalization of G was therefore most probably enforced by displacement of G owing to Gly 42 and not as a result of efficient N9-pathway reaction. The initiation of N9-pathway is conditioned by tight contact of Nε-ammonium with lone-pair electrons at glycosidic nitrogen that was apparently ensured only for the damaged nucleosides (Table S4).

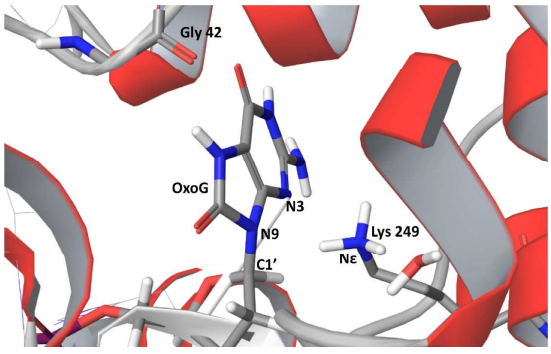

Figure 3. The positioning of OxoG nucleoside within hOGG1 catalytic pocket as was optimized employing large model. The Nε-ammonium of Lys 249 interacts with glycosidic nitrogen N9 of OxoG. The H-bond between oxygen of Gly 42 and H7 hydrogen of OxoG is key for proper stabilization of OxoG within catalytic site. For geometric parameters see the Table S4.

The Wiberg bond orders were calculated employing small models. The bond order of C1´-N9 bond of free G, OxoG and FapyG was 0.898, 0.924, and 0.971, respectively. The gradual strengthening of N-glycosidic bond was coherent with the bond shortening (Table 1). The bond order of C1´-N9 bond of OxoG owing to C1'-pathway, N3-pathway, and N9-pathway was 0.922, 0.923, 0.905, respectively. The degree of activation of C1´-N9 bond can be evaluated with the Wiberg bond orders because the activation energies of N-glycosidic bond cleavage calculated previously decreased in the same order as bond orders.[31] The activation of C1´-N9 bond owing to N9-pathway and particularly owing to N9-pathway with proton transferred to N9 was more efficient than activations owing to other two pathways (Table S5).

The NBO charges were calculated employing small model. The charge of N9 nitrogen of G, OxoG and FapyG ranged -0.420 ÷ -0.410 e, -0.474 ÷ -0.544 e, and -0.745 ÷ -0.645 e, respectively. The charge of C1' carbon ranged 0.244 ÷ 0.280 e and the charge of N3 nitrogen ranged -0.655 ÷ -0.590 e (Table S6 - Table S8). The interaction of N9 nitrogen with Nε-ammonium of Lys 249 was enhanced more in the case of damaged nucleosides as compared to normal G. The N3-pathway seemed to be competitive in that regard particularly in the case of OxoG. The effect of hOGG1 residues on proper mutual arrangement of Lys 249 with respect to nucleoside seemed indispensable.

The Fukui indices f^2 were calculated employing small model. The positive or negative value of f^2 unveiled electrophilic or nucleophilic character of atoms in nucleosides. The C1' carbon was slightly electrophilic (Table 2, Table S9 - Table S11). The N3 nitrogen was nucleophilic except the N3 of G with transferred proton owing to N3-pathway that was nucleophilic. The N9 nitrogen of G was electrophilic but the N9 of OxoG and FapyG was increasingly nucleophilic. Importantly, the glycosidic nitrogen atoms of nucleosides interacting with Lys 249 kept their inherent character, which was coherent with specificity of N9-pathway with respect to normal and damaged nucleosides. Particular character of the glycosidic nitrogen determined inherent propensity for interaction with electrophile (proton of Nε-ammonium) or nucleophile (Nε-amino group). The significant nucleophilicity allowed proton addition to N9 of FapyG. The electrophilicity of N9 of G caused ineffective initiation of N9-pathway. Similar discriminative role of N9 nitrogen was recently proposed for excision of hypoxanthine with alkyladenine DNA glycosylase repair enzyme.[37] The chemical hardness of G nucleoside was larger than chemical hardness of OxoG and FapyG (Table S12). The effect owing to electronic character of N9 on activation of N-glycosidic bond could be therefore amplified by increased reactivity of the damaged nucleosides.

Table 2. The Fukui indices f^2 calculated for C1', N9, and N3 atoms of G, OxoG and FapyG.[a)]

Atom	Free nucleoside	C1'-pathway	N3-pathway		N9-pathway	
	G	G (C1')	G (N3)	G (N3H)	G (N9)	G (N9H)
C1´	0.000	0.007	0.006	0.001	-	-
N9	0.020	-0.003	0.011	0.011	-	-
N3	-0.104	-0.117	-0.068	0.015	-	-
	OxoG	OxoG (C1')	OxoG (N3)	OxoG (N3H)	OxoG (N9)	OxoG (N9H)
C1´	0.003	0.007	0.008	0.005	0.004	-
N9	-0.013	-0.028	-0.029	-0.022	-0.017	-
N3	-0.048	-0.059	-0.046	-0.021	-0.080	-
	FapyG	FapyG (C1')	FapyG (N3)	FapyG (N3H)	FapyG (N9)	FapyG (N9H)
C1´	0.009	0.010	0.008	0.008	0.004	0.005
N9	-0.063	-0.092	-0.086	-0.080	-0.036	-0.006
N3	-0.034	-0.038	-0.041	-0.018	-0.077	-0.078

[a)] The numbering of atoms is depicted in Figure 1. The three pathways are indicated in parenthesis as follows: C1'-pathway (C1'), N3-pathway (N3), N3-pathway with proton transferred from Nε-ammonium to N3 nitrogen (N3H), N9-pathway (N9), N9-pathway with proton transferred from Nε-ammonium to N9 nitrogen (N9H). The calculations were done employing small model depicted in Figure 2 and described in Computational details. -: not calculated (see the text).

The nucleus-independent chemical shielding (NICS) is indicator of aromaticity.[38,39] The negative or positive NICS values computed at the ring center indicated its aromatic or anti-aromatic character (Figure S1). The character of five-membered ring of G was more aromatic than character of five-membered ring of OxoG (Table 3). The six-membered ring of G possessed less aromatic character than six-membered ring of OxoG. Interestingly, the decrease of aromaticity of five-membered ring owing to damage was balanced by aromaticity increase of the unmodified six-membered ring. The upmost decrease of aromaticity of five-membered ring of OxoG was calculated for N9-pathway, which was coherent with the depletion of electron density near N9 owing to less conjugated character of N9-C8 and N9-C4 inner-ring bonds (Table S5).

Table 3. The NICS values calculated for five- and six-membered ring of G, OxoG and FapyG.[a)]

NICS	Free nucleoside	C1'-pathway	N3-pathway		N9-pathway	
	G	G (C1')	G (N3)	G (N3H)	G (N9)	G (N9H)
NICS-5	-12.5	-11.6	-12.0	-12.8	-	-
NICS-6	-4.4	-4.2	-3.8	-3.9	-	-
	OxoG	OxoG (C1')	OxoG (N3)	OxoG (N3H)	OxoG (N9)	OxoG (N9H)
NICS-5	-10.5	-10.9	-10.7	-10.9	-9.1	-
NICS-6	-4.9	-4.7	-4.0	-4.2	-4.3	-
	FapyG	FapyG (C1')	FapyG (N3)	FapyG (N3H)	FapyG (N9)	FapyG (N9H)
NICS-6[b)]	-1.3	-1.3	-0.7	-0.7	-0.5	-0.8
NICS-6	-3.9	-3.2	-3.2	-4.0	-4.1	-3.8

[a)] The nucleus independent chemical shielding NICS-5 and NICS-6 in ppm were calculated at the centre of mass of five- and six-membered ring of nucleobases. [b)] The NICS-6 values calculated for six-membered pseudo-ring of FapyG containing glycosidic nitrogen N9. The interaction of Lys 249 with nucleosides are indicated in parenthesis as follows: C1'-pathway (C1'), N3-pathway (N3), N3-pathway with proton

transferred from Nε-ammonium to N3 nitrogen (N3H), N9-pathway (N9), N9-pathway with proton transferred from Nε-ammonium to N9 nitrogen (N9H). The calculations were done employing small model (Figure 2) as described in Computational details. -: not calculated (see the text).

The N3-pathway and N9-pathway were compared by means of calculated interaction energies. The absolute values of ΔE_{int} energies calculated for N3-pathway were larger than the energies for N9-pathway (Table 4), which was coherent with respective bond orders. The H-N3 bond orders calculated for H atom of Nε-ammonium and N3 nitrogen of nucleosides owing to N3-pathway were larger than the H-N9 bond orders owing to N9-pathway (Table S5). The interaction of Nε-ammonium with N3 nitrogen was better energy-stabilized than the interaction with N9 nitrogen. On the other hand, the N9-pathway was stabilized increasingly better for the damaged nucleosides while the N3-pathway was in that regard more conservative owing to distinct electrophilicity of N3. The interaction of Lys 249 with N9 nitrogen depended on character of N9 nitrogen. The more distinct was nucleophilic character of glycosidic nitrogen the more stable was its interaction with Nε-ammonium. Importantly, the interaction of Nε-ammonium with N9 atom of OxoG is stabilized energetically owing to negative interaction energy.

Table 4. The interaction energies calculated for G, OxoG and FapyG nucleosides interacting with Lys 249.

Nucleoside (pathway) [a)]	ΔE_{int} [b)]
G (N3)	-8.3
OxoG (N3)	-7.6
OxoG (N9)	-2.5
FapyG (N3)	-11.0
FapyG (N9)	-9.8

[a)] The N3-pathway and N9-pathway are depicted for OxoG in Figure 2. [b)] The interaction energy ΔE_{int} in kcal mol^{-1} was calculated as energy of small model minus energy of monomers (Lys 249, nucleoside) including the basis set superposition error (BSSE). The BSSE represented ca 1 kcal mol^{-1} and calculation details are described in the Table S13.

The specific activation of N-glycosidic bond of G, OxoG, and FapyG was calculated because normal and damaged nucleosides possessed characteristic structural and electronic properties. When going from G to OxoG and to FapyG the C1´-N9 bond shrank, the respective bond order increased, the charge of N9 nitrogen decreased, the lone-pair electrons at N9 were more localized (Figure S2), the aromaticity of five-membered ring decreased and the character of glycosidic nitrogen changed from electrophilic to nucleophilic.

The activation of N-glycosidic bond employing C1'-pathway was relatively unspecific as compared to N3-pathway or N9-pathway. The Gibbs free energy of cleavage of N-glycosidic bond of G, OxoG, and FapyG calculated employing C1'-pathway was 30.7, 32.0 and 35.2 kcal mol^{-1}, respectively. (Small model, Table S14, Figure S3.) The $\Delta G^{\#}$ energies thus increased in the same order as increased the respective C1´-N9

bond orders. This indicated rather dependence of activation on strength of the bond than significant activation role of Lys 249. Actually, the N-glycosidic bond of G is more labile toward hydrolytic cleavage than N-glycosidic bond of OxoG.[40] The minor activation role of Lys 249 in calculations employing C1'-pathway can be therefore assumed. The hydrolytic and enzymatic cleavage apparently proceed according to different scenarios. The calculated activation employing C1'-pathway was in conflict with the observed cleavability of G and OxoG operated by hOGG1.[18,17,34,28]

The protonation of N9 and N3 atoms owing to N9-pathway and N3-pathway depended on degree of their nucleophilicity. The proton addition to N3 nitrogen was calculated for all three nucleosides while the proton addition to N9 nitrogen was calculated only for FapyG. The Gibbs free activation and reaction energies calculated for transfer of proton from Nε-ammonium to N3 or N9 nitrogen indicated that proton transfer to N3 nitrogen of G should be easier and better stabilized than proton transfer to N3 or N9 of OxoG and FapyG (Table S14, Figure S4, Figure S5). The activation energies calculated for proton transfer were nevertheless quite similar and N3-pathway reaction may probably result in pre-protonation of N3 nitrogen and N9 nitrogen of FapyG.

The activation operated by hOGG1 employs some mechanism that activates specifically the intrinsically more stable N-glycosidic bond of damaged nucleosides. The N9-pathway was specific in that regard but the "net" interaction of Lys 249 with glycosidic nitrogen was only loosely stabilized. The workability of relatively fragile N9-pathway was conditioned by nucleophilic character of glycosidic nitrogen and by hOGG1 catalytic site that ensured effective attack of lone-pair electrons at glycosidic nitrogen to proton of Nε-ammonium by proper deposition of damaged nucelosides (Figure S6). The N9-pathway may be regarded typical enzymatic strategy because its workability was strictly conditioned by arrangement of catalytic core and distinct character of a substrate nucleoside.

Conclusions

The activation N-glycosidic bond employing Lys 249 residue of hOGG1 enzyme was calculated for normal G, OxoG and FapyG nucleosides. The activation of N-glycosidic bond operated by attack of lone-pair electrons at glycosidic nitrogen to Nε-ammonium of Lys 249 was efficient and specific with respect to normal and damaged nucleosides. The activation of normal G initiated by N9-pathway reaction was ineffective owing to electrophilic character of glycosidic nitrogen of G and corrupted catalytic core that contained displaced substrate. The activation of the damaged nucleosides was effective owing to nucleophilic character of glycosidic nitrogen and favorable mutual arrangement of nucleoside with respect to Lys 249. The glycosidic nitrogen of both OxoG and FapyG can donate lone-pair electrons capable of interaction with proton of Nε-ammonium of Lys 249 while the lone-pair electrons at N9 of G can't interact efficiently with Nε-ammonium owing to their delocalization within five-membered ring.

The interaction of protonated Lys 249 with electrophilic or nucleophilic glycosidic nitrogen triggered specific activation of N-glycosidic bond of normal and damaged nucleosides that could be involved as a check-point mechanism during base-excision operated by hOGG1. We therefore propose that Lys 249 is not only key catalytic residue, but also the residue involved in recognition of damaged nucleobases.

Computational details

Three structural models called small, medium and large were employed. The small model that was derived employing the x-ray structure 1N3C[17] consisted of nucleoside and Lys 249 (Figure 2). Mutual positioning of the residues was constrained by fixed geometries of C4′ and C3′ atoms of nucleoside and -OCCN- atoms of Lys 249. The B3LYP-D2 method including Grimme's dispersion corrections D2[41,42,43], the 6-31G(d,p)[44,45] basis set, and the PCM solvent (diethylether) were employed in geometry optimizations. The PCM method was used successfully to mimic overall polarization within catalytic site in similar studies.[46,47,48] The energy minima and transition states were confirmed by vibrational frequency analysis. The free nucleosides (not interacting with Lys 249) were optimized without constraints. The medium model that was derived employing the x-ray structure 2NOZ[19] included nucleoside and hOGG1 residues within 10 Å sphere centred at glycosidic nitrogen of nucleoside (Figure 4). The Lys 249, Asp 268, Cys 253, Phe 319, W2979, W2908, W2907 water molecules, and nucleoside defined the inner part within ONIOM QM/QM[49] method that was optimized employing the CAM-B3LYP DFT method[50] while the outer part (650 atoms) was optimized employing the PM6 method keeping the heavy atoms fixed. The small and medium models of G and FapyG were derived using the original x-ray structures that included OxoG and by keeping the maximal overlap of nucleobases. The large model was derived employing 2NOZ x-ray structure that described hOGG1-DNA complex (Figure 5). Only the DNA heptamer including OxoG in the middle was included in large model. The OxoG and neighbouring nucleotides within DNA strand and hOGG1 protein were geometry optimized while the rest of heavy atoms of DNA heptamer were kept fixed in their x-ray geometries. The QM/MM AM1[51]/OPLS_2005[52] and B3LYP(6-31G(d,p))/OPLS_2005 methods within additive scheme were employed in geometry optimizations of large model. The hydrogen cap and electrostatic treatment at the QM/MM interface using Gaussian charge distribution on a grid was employed. The QM part of large model included OxoG nucleoside and Lys 249, Gly 42, and Gln 43 residues of hOGG1. The protonated form of Lys 249 was involved in both medium and large model.

The calculated N9-pyramidalizations (κ' = 27.7°÷48.2°) were larger than N9-pyramidalizations in x-ray structures (κ' = -0.3°÷2.8°). The ultra-high resolution of x-ray structures (resolution of 1 Å or better and R-factor < 0.2) is required because lower resolution that is often linked with usage of empirical force-field may result in underestimated N9-pyramidalization.[32] The resolutions of 3IH7[28], 1YQK[53], 1N3C[17], 2NOZ[19] x-ray structures ranged 2.43 Å÷3.10 Å and the N9-pyramidalizations might be therefore underestimated.

The molecular properties calculated employing small models included geometry, natural bond orbital (NBO) atomic charges, natural localized molecular orbitals (NLMOs), Fukui functions[54,55] chemical hardness[56,57], interaction energies, bond orders, Wiberg bond indexes[58], nucleus independent chemical shifts (NICSs)[59,38,60], and Gibbs free activation and reaction energies. The NICSs were calculated employing B3LYP/6-31G(d,p) method. The interaction energies were calculated employing B3LYP-D2/6-311++G** method including the BSSE correction. All other properties were calculated employing B3LYP-D2/6-31G(d,p) method. Further details can be found in the Supporting Information.

The Fukui index of atom in a molecule $f^2 = f^+ - f^-$ was calculated as difference of Fukui functions $f^- = q(N-1) - q(N)$ and $f^+ = q(N) - q(N+1)$ where the q(N-1), q(N), q(N) were atomic

NBO charges of molecule containing N-1, N, and N+1 electrons, respectively. The global reactivity descriptor of a molecule $\eta = \frac{1}{2}\left(\varepsilon_{LUMO} - \varepsilon_{HOMO}\right)$ called chemical hardness was calculated employing electronic energies of the LUMO and HOMO molecular orbitals.

The small and medium models were geometry optimized using the Gaussian 09 program.[61] The large model was optimized using the QSite program.[62] The NBO atomic charges, NLMO orbitals and the Wiberg bond indexes were calculated within the NBO analysis[63] using the NBO program 3.1.[64].

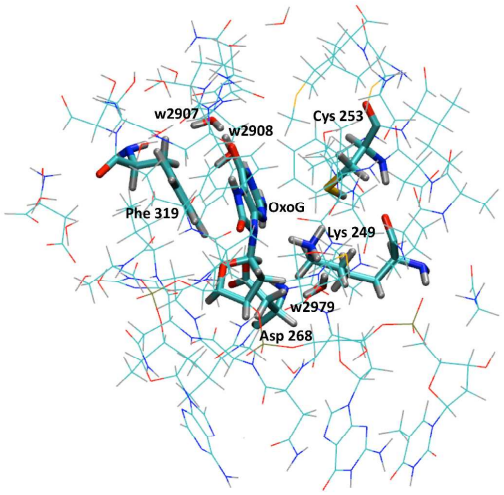

Figure 4. The medium structural model.

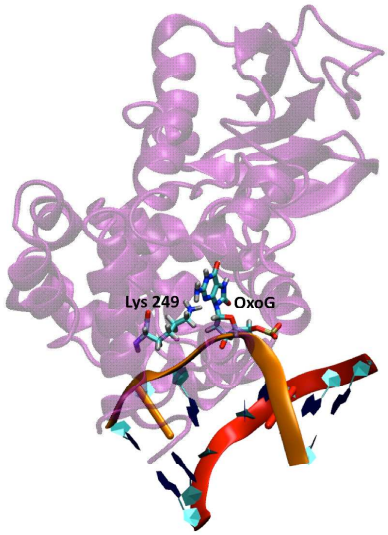

Figure 5. The large structural model.

Acknowledgement

This work was supported by the Czech Science Foundation GA ČR, grant number 13-27676S and by the Academy of Sciences, grant number M200551205. Y.T. and V.S. acknowledge the Young Investigator's Grant of the Human Frontier Science Program (HFSP). L.T. was supported by the project "CEITEC - Central European Institute of Technology" (CZ.1.05/1.1.00/02.0068) from European Regional Development Fund and from the European Social Fund and the state budget of the Czech Republic (CZ.1.07/2.3.00/20.0042).

References

1. P. J. Berti and J. A. B. McCann, *Chemical Reviews*, 2006, 106, 506-555.
2. S. S. David and S. D. Wiliams, *Chemical Reviews*, 1998, 98, 1221-1261.
3. H. M. Nash, S. D. Bruner, O. D. Scharer, T. Kawate, T. A. Addona, E. Sponner, W. S. Lane and G. L. Verdine, *Curr. Biol.*, 1996, 6, 968-980.
4. M. Bjoras, L. Luna, B. Johnson, E. Hoff, T. Haug, T. Rognes and E. Seeberg, *Embo J.*, 1997, 16, 6314-6322.
5. H. M. Nash, R. Z. Lu, W. S. Lane and G. L. Verdine, *Chemistry & Biology*, 1997, 4, 693-702.
6. R. Z. Lu, H. M. Nash and G. L. Verdine, *Curr. Biol.*, 1997, 7, 397-407.
7. S. Boiteux and J. P. Radicella, *Archives of Biochemistry and Biophysics*, 2000, 377, 1-8.
8. M. D. Leipold, J. G. Muller, C. J. Burrows and S. S. David, *Biochemistry*, 2000, 39, 14984-14992.
9. K. Shinmura and J. Yokota, *Antioxid. Redox Signal.*, 2001, 3, 597-609.
10. H. Menoni, M. S. Shukla, V. Gerson, S. Dimitrov and D. Angelov, *Nucleic Acids Res.*, 2012, 40, 692-700.
11. S. S. David, V. L. O'Shea and S. Kundu, *Nature*, 2007, 447, 941-950.
12. P. L. McKibbin, A. Kobori, Y. Taniguchi, E. T. Kool and S. S. David, *Journal of the American Chemical Society*, 2012, 134, 1653-1661.
13. Y. W. Kow and S. S. Wallace, *Biochemistry*, 1987, 26, 8200-8206.
14. M. L. Dodson, M. L. Michaels and R. S. Lloyd, *J. Biol. Chem.*, 1994, 269, 32709-32712.
15. J. T. Stivers and Y. L. Jiang, *Chemical Reviews*, 2003, 103, 2729-2759.
16. S. D. Bruner, D. P. G. Norman and G. L. Verdine, *Nature*, 2000, 403, 859-866.
17. D. P. G. Norman, S. J. Chung and G. L. Verdine, *Biochemistry*, 2003, 42, 1564-1572.
18. J. C. Fromme, S. D. Bruner, W. Yang, M. Karplus and G. L. Verdine, *Nature Structural Biology*, 2003, 10, 204-211.
19. C. T. Radom, A. Banerjee and G. L. Verdine, *J. Biol. Chem.*, 2007, 282, 9182-9194.
20. T. Osakabe, Y. Fujii, M. Hata, M. Tsuda, S. Neya and T. Hoshino, *Chem-Bio Informatics Journal* 2004, 4, 73-92.
21. P. Schyman, J. Danielsson, M. Pinak and A. Laaksonen, *Journal of Physical Chemistry A*, 2005, 109, 1713-1719.
22. J. A. B. McCann and P. J. Berti, *Journal of the American Chemical Society*, 2008, 130, 5789-5797.
23. A. L. Millen and S. D. Wetmore, *Can. J. Chem.-Rev. Can. Chim.*, 2009, 87, 850-863.

24. E. J. Shim, J. L. Przybylski and S. D. Wetmore, *Journal of Physical Chemistry B*, 2010, 114, 2319-2326.
25. R. Rios-Font, J. Bertran, M. Sodupe and L. Rodriguez-Santiago, *Theoretical Chemistry Accounts*, 2011, 128, 619-626.
26. J. L. Kellie and S. D. Wetmore, *Journal of Physical Chemistry B*, 2012, 116, 10786-10797.
27. A. A. Kuznetsova, N. A. Kuznetsov, A. A. Ishchenko, M. K. Saparbaev and O. S. Fedorova, *Biochim. Biophys. Acta-Gen. Subj.*, 2014, 1840, 387-395.
28. C. M. Crenshaw, N. Kwangho, O. Kimberly, P. S. Kutchikian, B. Bowman, M. Karplus and G. L. Verdine, *J. Biol. Chem.*, 2012, 287, 24916-24928.
29. P. J. O'Brien, *Chemical Reviews*, 2006, 106, 720-752.
30. M. Calvaresi, A. Bottoni and M. Garavelli, *Journal of Physical Chemistry B*, 2007, 111, 6557-6570.
31. J. Sebera, L. Trantirek, Y. Tanaka and V. Sychrovsky, *Journal of Physical Chemistry B*, 2012, 116, 12535-12544.
32. V. Sychrovsky, S. Foldynova-Trantirkova, N. Spackova, K. Robeyns, L. Van Meervelt, W. Blankenfeldt, Z. Vokacova, J. Sponer and L. Trantirek, *Nucleic Acids Res.*, 2009, 37, 7321-7331.
33. V. Sychrovsky, Z. S. Vokacova and L. Trantirek, *Journal of Physical Chemistry A*, 2012, 116, 4144-4151.
34. C. Dherin, J. P. Radicella, M. Dizdaroglu and S. Boiteux, *Nucleic Acids Res.*, 1999, 27, 4001-4007.
35. Y. H. Jang, W. A. Goddard, K. T. Noyes, L. C. Sowers, S. Hwang and D. S. Chung, *Chem. Res. Toxicol.*, 2002, 15, 1023-1035.
36. P. Cysewski, D. Bira and K. Bialkowski, *Journal of Molecular Structure-Theochem*, 2004, 678, 77-81.
37. X. Sun and J. K. Lee, *J. Org. Chem.*, 2007, 72, 6548-6555.
38. Z. Chen, Heine T., Schelyer P. R., Sundholm D., in *Calculation of NMR and EPR Parameters*, ed. M. B. M. Kaupp, V.G. Malkin, WILEY-VCH Verlag, 2004.
39. Z. F. Chen, C. S. Wannere, C. Corminboeuf, R. Puchta and P. V. Schleyer, *Chemical Reviews*, 2005, 105, 3842-3888.
40. K. Bialkowski, P. Cysewski and R. Olinski, *Z.Naturforsch.(C)*, 1996, 51, 119-122.
41. A. D. Becke, *J. Chem. Phys.*, 1993, 98, 5648-5652.
42. C. T. Lee, W. T. Yang and R. G. Parr, *Physical Review B*, 1988, 37, 785-789.
43. S. Grimme, *Journal of Computational Chemistry*, 2006, 27, 1787-1799.
44. W. J. Hehre, Ditchfie.R and J. A. Pople, *J. Chem. Phys.*, 1972, 56, 2257-&.
45. Harihara.Pc and J. A. Pople, *Theor. Chim. Acta*, 1973, 28, 213-222.
46. J. Tomasi, B. Mennucci and R. Cammi, *Chemical Reviews*, 2005, 105, 2999-3093.
47. S. C. Harvey and P. Hoekstra, *Journal of Physical Chemistry*, 1972, 76, 2987-&.
48. G. King, F. S. Lee and A. Warshel, *J. Chem. Phys.*, 1991, 95, 4366-4377.
49. T. Vreven, K. S. Byun, I. Komaromi, S. Dapprich, J. A. Montgomery, Jr., K. Morokuma and M. J. Frisch, *Journal of Chemical Theory and Computation*, 2006, 2, 815-826.
50. T. Yanai, D. P. Tew and N. C. Handy, *Chemical Physics Letters*, 2004, 393, 51-57.
51. M. J. S. Dewar, E. G. Zoebisch, E. F. Healy and J. J. P. Stewart, *Journal of the American Chemical Society*, 1985, 107, 3902-3909.

52. W. L. Jorgensen, D. S. Maxwell and J. TiradoRives, *Journal of the American Chemical Society*, 1996, 118, 11225-11236.
53. A. Banerjee, W. Yang, M. Karplus and G. L. Verdine, *Nature*, 2005, 434, 612-618.
54. W. Yang and W. J. Mortier, *Journal of the American Chemical Society*, 1986, 108, 5708-5711.
55. C. Morell, A. Grand and A. Toro-Labbe, *Journal of Physical Chemistry A*, 2005, 109, 205-212.
56. P. D. P. Geerlings, F.; Martin, J. M. L. , Theoretical and Computational Chemistry 4, Elsevier, 1996, p. 773.
57. P. Geerlings, F. De Proft and W. Langenaeker, *Chemical Reviews*, 2003, 103, 1793-1873.
58. K. B. Wiberg, *Tetrahedron*, 1968, 24, 1083-1096.
59. P. V. Schleyer, C. Maerker, A. Dransfeld, H. J. Jiao and N. Hommes, *Journal of the American Chemical Society*, 1996, 118, 6317-6318.
60. S. Pelloni, G. Monaco, P. Lazzeretti and R. Zanasi, *Physical Chemistry Chemical Physics*, 2011, 13, 20666-20672.
61. Gaussian 09, Revision B.02, M. J. Frisch, G. W. Trucks, H. B. Schlegel, G. E. Scuseria, M. A. Robb, J. R. Cheeseman, G. Scalmani, V. Barone, B. Mennucci, G. A. Petersson, H. Nakatsuji, M. Caricato, X. Li, H. P. Hratchian, A. F. Izmaylov, J. Bloino, G. Zheng, J. L. Sonnenberg, M. Hada, M. Ehara, K. Toyota, R. Fukuda, J. Hasegawa, M. Ishida, T. Nakajima, Y. Honda, O. Kitao, H. Nakai, T. Vreven, J. A. Montgomery, Jr., J. E. Peralta, F. Ogliaro, M. Bearpark, J. J. Heyd, E. Brothers, K. N. Kudin, V. N. Staroverov, R. Kobayashi, J. Normand, K. Raghavachari, A. Rendell, J. C. Burant, S. S. Iyengar, J. Tomasi, M. Cossi, N. Rega, J. M. Millam, M. Klene, J. E. Knox, J. B. Cross, V. Bakken, C. Adamo, J. Jaramillo, R. Gomperts, R. E. Stratmann, O. Yazyev, A. J. Austin, R. Cammi, C. Pomelli, J. W. Ochterski, R. L. Martin, K. Morokuma, V. G. Zakrzewski, G. A. Voth, P. Salvador, J. J. Dannenberg, S. Dapprich, A. D. Daniels, Ö. Farkas, J. B. Foresman, J. V. Ortiz, J. Cioslowski, and D. J. Fox, Gaussian, Inc., Wallingford CT, 2009.
62. QSITE, v. 6.1; Schroedinger, LLC: New York, 2013.
63. A. E. Reed, L. A. Curtiss and F. Weinhold, *Chemical Reviews*, 1988, 88, 899-926.
64. E. D. Glendening, A. E. Reed, J. E. Carpenter and F. Weinhold, *Theoretical Chemistry Institute, University of Wisconsin*.